

Simple, General, Realistic, Robust, Analytic, Tokamak Equilibria: Numerical Evaluation

L. Guazzotto^{1,*} and J. P. Freidberg²

¹Physics Department, Auburn University, Auburn, AL, 36849

²Plasma Science and Fusion Center, Massachusetts Institute of Technology, Cambridge, MA 02139 USA

1. The Model This work describes some additional details regarding the numerical evaluation of the analytic solution for the Grad-Shafranov (GS) equation introduced in Refs. [1-2]. The reader is directed to Refs. [1-2] for further details on the analytic solution, which will only be briefly summarized here, and for general references on analytic solutions of the GS equation. Before reviewing the main aspect of the solution in Refs. [1-2], we will remind the reader that the importance of analytic solutions of the GS equation is in their use for analytical studies (for instance of stability problems) and for benchmarking numerical codes. In this second aspect it becomes important to be able to evaluate accurately the numerical value of the solution in any desired point. This may be trivial for solutions with very simple functional forms, such as polynomials, but will become more challenging when special functions, such as Whittaker functions, are involved in the solution. The study of the convergence of our numerical evaluation of the solution in different situations is the purpose of the present work. We emphasize that the solution itself is analytic and as such does not require any convergence study. What follows is only meant to apply to the numerical evaluation.

Coming now to the solution approach, we start from the well-known static GS equation:

$$R \frac{\partial}{\partial R} \left(\frac{1}{R} \frac{\partial \Psi}{\partial R} \right) + \frac{\partial^2 \Psi}{\partial Z^2} = -\mu_0 R^2 \frac{dp}{d\Psi} - \frac{1}{2} \frac{dF^2}{\partial \Psi}. \quad (1)$$

The free functions are defined as

$$p(\Psi) = p_0 \left(\frac{\Psi}{\Psi_0} \right)^2, \quad F^2(\Psi) = R_0^2 B_0^2 \left[1 + \frac{2\delta B}{B_0} \left(\frac{\Psi}{\Psi_0} \right)^2 \right]. \quad (2)$$

With the definitions in Eq. (2), the GS equation is linear. It is convenient to cast it in non-dimensional form by setting

$$Z = ay, \quad R = R_0 r^{1/2} = R_0 (1 + \epsilon^2 + 2\epsilon x)^{1/2}, \quad -1 < x < 1. \quad (3)$$

Using the dimensionless variables x and y , we obtain the dimensionless form of the GS equation:

$$(1 + \hat{\epsilon}x) \frac{\partial^2 \psi}{\partial x^2} + \frac{1}{1 + \epsilon^2} \frac{\partial^2 \psi}{\partial y^2} = -\alpha^2 (1 + \hat{\epsilon} \nu x) \psi, \quad \psi_{\text{surface}} = 0. \quad (4)$$

*Author to whom correspondence should be addressed. Email: luca.guazzotto@auburn.edu

In Eq. (4) we have defined

$$\hat{\epsilon} = \frac{2\epsilon}{1+\epsilon^2} < 1, \quad \alpha^2 = \frac{2R_0^2 a^2}{\Psi_0^2} \left(\mu_0 p_0 + \frac{B_0 \delta B}{1+\epsilon^2} \right) \geq 0 \quad (\text{eigenvalue}) \quad (5)$$

$$\nu = \frac{\mu_0 p_0}{\mu_0 p_0 + B_0 \delta B / (1+\epsilon^2)} \simeq \beta_p \geq 0. \quad (6)$$

The standard form of the GS equation and its boundary condition were extended in Ref. [2] to include toroidal rotation and edge discontinuities, including surface currents and jumps of pressure and toroidal current. If toroidal rotation is included, the GS equation becomes:

$$(1 + \hat{\epsilon}x) \frac{\partial^2 \psi}{\partial x^2} + \frac{1}{1 + \epsilon^2} \frac{\partial^2 \psi}{\partial y^2} = -\alpha^2 [1 + \nu G(x)] \psi, \quad (7)$$

$$G(x) = (1 + \hat{\epsilon}x) \left(1 + \frac{2M_0^2 \epsilon}{1 + M_0^2 \epsilon^2} x \right)^{\frac{\gamma}{\gamma-1}} - 1, \quad (8)$$

where M_0 is a Mach number; ν and α are also modified by the flow. An analytic solution can be written for $\gamma = n/(n-1)$, where $n \in \mathbb{N}$. We focus on $\gamma = 2$ and $\gamma \rightarrow \infty$. As for pedestals, introducing (1) a pressure jump at the edge (\sim “pressure pedestal”) and (2) an edge-localized bootstrap current (surface current) does not modify the solution of Eq. (7). Rather, one only needs to modify the post-processing expressions for physical quantities of interest (e.g. β_p , q_*). The discontinuities are determined by the input parameters f_P and f_B , defined as follows: For the pressure pedestal, $p_{\text{edge}}/p_0 = f_P < 1$, while for the bootstrap fraction: $I_{\text{total}} = I_{\text{core}} + I_{\text{bootstrap}}$ and $f_B = I_{\text{bootstrap}}/I_{\text{total}}$. Note that if $f_B \neq 0$ the edge jump in B_φ between plasma and vacuum sides must be calculated numerically to satisfy total pressure continuity. The situation is a little different if a finite edge value for $\langle J_\varphi \rangle$ is also allowed. In that case, the free functions are modified to:

$$p = p_0 \{ f_P + (1 - f_P) \psi^2 + A_1 [\psi - \psi^2] \}, \quad (9)$$

$$F^2 = R_0^2 B_0^2 \left\{ 1 + \frac{2\delta B}{B_0} \psi^2 + 2A_2 [\psi - \psi^2] \right\}. \quad (10)$$

It is expedient to set the constants A_1 and A_2 as:

$$A_1 = \frac{2(1 - f_P) f_J}{1 + f_J}, \quad A_2 = \frac{\delta B}{B_0} \frac{A_1}{1 - f_P}. \quad (11)$$

This leaves the GS equation formally unchanged up to some modifications of ν and α . However, the boundary condition is now

$$\psi_{\text{new}}(\text{surf}) = \frac{f_J}{1 - f_J}. \quad (12)$$

2. The Solution Regardless of the level of complication included in the model, the solution strategy is the same. Using separation of variables we write $\psi(x, y) = \sum_n X_n(x) Y_n(y)$. The equations to be solved are

$$\frac{d^2 Y_n}{dy^2} + h_n^2 Y_n = 0 \quad \rightarrow \quad Y_n = \cos(h_n y), \sin(h_n y); \quad (13)$$

$$(1 + \hat{\epsilon}x) \frac{d^2 X_n}{dx^2} + (k_n^2 + \lambda_1^2 x + \lambda_2^2 x^2 + \lambda_3^2 x^3) X_n = 0. \quad (14)$$

We used the separation constants

$$h_n^2 \rightarrow \text{separation constants, } k_n^2 = \alpha^2 - \frac{h_n^2}{1 + \epsilon^2} \quad (15)$$

The polynomial (in x) aspect of the linear (in X_n) term in Eq. (14) is due to the special choice made for γ . The constants λ_j have simple relations with ν and M_0 , given in Ref. [2]. In particular $\lambda_3 = 0$ if $\gamma \rightarrow \infty$. The next step is to find a series expansion of the function X_n . For the static case, X_n can be expressed in terms of Whittaker functions, but that has no effect on the rest of our work. The key intuition is to make all of the h_n^2 and k_n^2 positive. Then the solution for each value of n will form closed curves around and in the proximity of the geometric axis. By writing

$$X_n(x) = \sum_{m=0}^{\infty} [a_m x^m \cos(k_n x) + b_m x^m \sin(k_n x)] \quad (16)$$

the calculation of X_n converges quickly, guaranteeing a \sim sine or cosine behavior for each solution. Different initial values in the recursion relations for a_m and b_m are used for the two independent solutions $C_n(x)$, $S_n(x)$ for each n . This gives the general form

$$\psi(x, y) = \sum_n \cos(h_n y) [c_{n,1} C_n(x) + s_{n,1} S_n(x)] + \sum_n \sin(h_n y) [c_{n,2} C_n(x) + s_{n,2} S_n(x)] \quad (17)$$

for the solution. We pick the number of separation constants based on the minimum number of conditions needed to define the plasma shape. Fixing the value of ψ , curvature and X-point/maximum/minimum of the shape in appropriate points, we obtain 7 constraints for symmetric (smooth or double null) shapes, 12 for the single null shape. Given the number of constraints, we always use **four** values for h_n (16 constants total). For the **symmetric case**, all $c_{n,2}$ and $s_{n,2}$ are 0 (8 constant total). We set $h_1 = \alpha\sqrt{1 + \epsilon^2} \rightarrow k_1 = 0$ to make $S_1(x) = 0$ (7 constants total, as needed). For the **asymmetric case**, still set $h_1 = \alpha\sqrt{1 + \epsilon^2}$ ($k_1 = 0$, get rid of $s_{1,1}$ and $s_{1,2}$) and $h_4 = 0$ (get rid of $c_{4,2}$ and $s_{4,2}$). This leaves 12 constants to be determined, as needed. To satisfy all our conditions, we always pick the same h_n/k_n :

$$k_1 = 0, \quad k_2 = \frac{\alpha}{6}, \quad k_3 = \frac{6}{7}\alpha, \quad k_4 = \alpha, \quad (18)$$

which we have found to work surprisingly well for all the plasma shapes we have considered in our work. Note that it is easy to obtain the corresponding h_n from Eq. (15). The c_n and s_n constants and the eigenvalue α are determined imposing the boundary conditions.

3. The Numerical Evaluation Even though the solution is completely analytic, a numerical evaluation is needed to find the eigenvalue α and to represent the solution and compare it with numerical solutions obtained from GS solvers. Determining α requires to solve a relatively straightforward root-finding problem. This can be accomplished with prepackaged numerical tools. It is worthwhile to point out that the solution in Eq. (17) is an exact solution of the GS equation regardless of the value of α . Picking the correct value of α is required only to satisfy the boundary conditions. What requires some more attention is the number of terms needed to have an accurate evaluation of the solution. Depending on the application, different accuracies and therefore different numbers of terms may be desired.

We have written a MATLAB code to calculate and plot the solution. The code is freely available (email Luca Guazzotto at luca.guazzotto@auburn.edu) and will soon be uploaded on

<https://www.auburn.edu/cosam/faculty/physics/guazzotto/research/index.html>

We have used our numerical code to test convergence in the numerical evaluation of Eq. (17). We considered two shapes, labeled “case 3” (for a regular smooth tokamak) and “case 7” (for a spherical tokamak DN shape) in Fig. 1. We show results for a static case with no pedestals for the regular tokamak and for a case with all allowed pedestals and high rotation for the ST. We computed the solution for a number of terms in the series

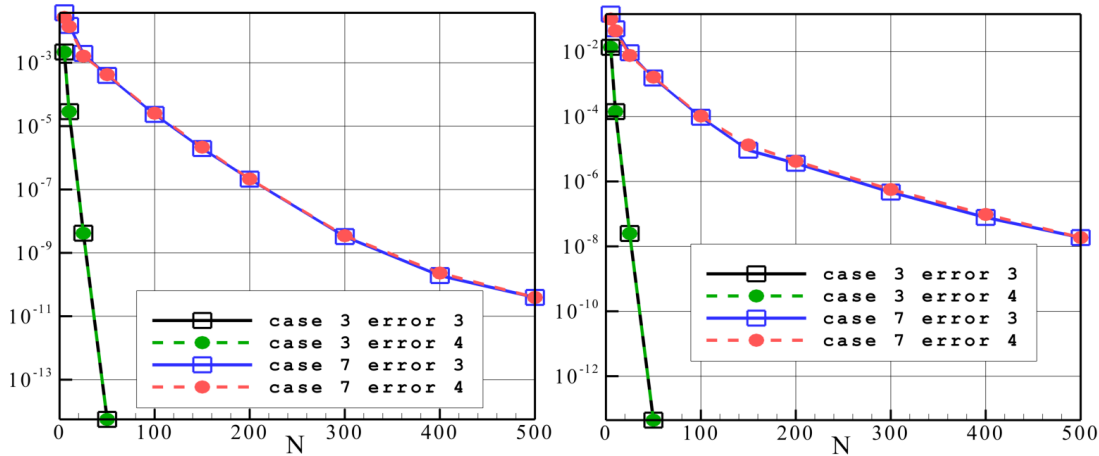


Figure 1: Average (left) and maximum (right) errors as defined in the text.

equal to 5, 10, 25, 50, 100, 150, 200, 300, 400, 500 and 1,000. We defined the “error 3” as the absolute value of the difference between ψ obtained using a given number of terms and ψ obtained using the next number of terms in the sequence. “Error 4” is defined similarly, but always using ψ obtained with 1,000 terms as reference. We also defined two similar errors, 1 and 2, which are the square of the errors 3 and 4, but we are not showing them since they are similar to the ones in Fig. 1. Note that ψ is dimensionless, so all the definitions above are also dimensionless. For simplicity, we calculated and compared ψ in 150,000 points on a square grid surrounding the required shape of the plasma. This makes the test more pessimistic than needed, since the largest differences are found outside the plasma. We have repeated the calculation for 21 different combinations of flows and pedestals for both shapes and obtained results similar to the ones in Fig. 1. This brings us to conclude that the geometry is the most important factor in determining the number of terms needed for convergence. A last point of interest is the fact that the time required to compute the solution increases rather slowly with the number of terms in the series, going up by about a factor of 3 to 6 (depending on the case) going from 5 to 1,000 terms in the series. The longest time needed for a case was \sim 30 seconds on a 2015 MacBook Pro. This efficiency is mostly due to the fact that MATLAB is well suited for this type of calculation and is a useful property of our code.

References

1. L. Guazzotto and J. P. Freidberg, J. Plasma Phys. **87** 905870303 (2021)
2. L. Guazzotto and J. P. Freidberg, J. Plasma Phys. **87** 905870305 (2021)